Measuring the Soft X-Ray Emission Area of Water Window LPP Light Sources Using Deconvolution

Ruairí Brady

Ruairí Brady, Kevin Mongey, Ben Delaney, Emma Sokell, Fergal O'Reilly
School of Physics, Science Centre North, University College Dublin, Ireland

Abstract

Laser produced plasma (LPP) sources with emission diameters below 10 μm have been used to produce relatively high radiance levels in the soft x-ray (SXR) region [1]. These sources are suitable for applications such as SXR microscopy, where biological specimen are imaged with nanometer resolution using SXRs in the water window (WW) region [2]. One major line of research in the UCD Spectroscopy group involves driving down the emission volume of LPPs to increase their radiance. However, calculating the radiance of these sources proves challenging as any attempt to image them using a pinhole will be distorted due to diffraction. To counteract these effects and reveal their true shape and size, a model was developed which deconvolves images of LPPs with $1/e^2$ widths in the micrometer scale.

1. LPP Imaging

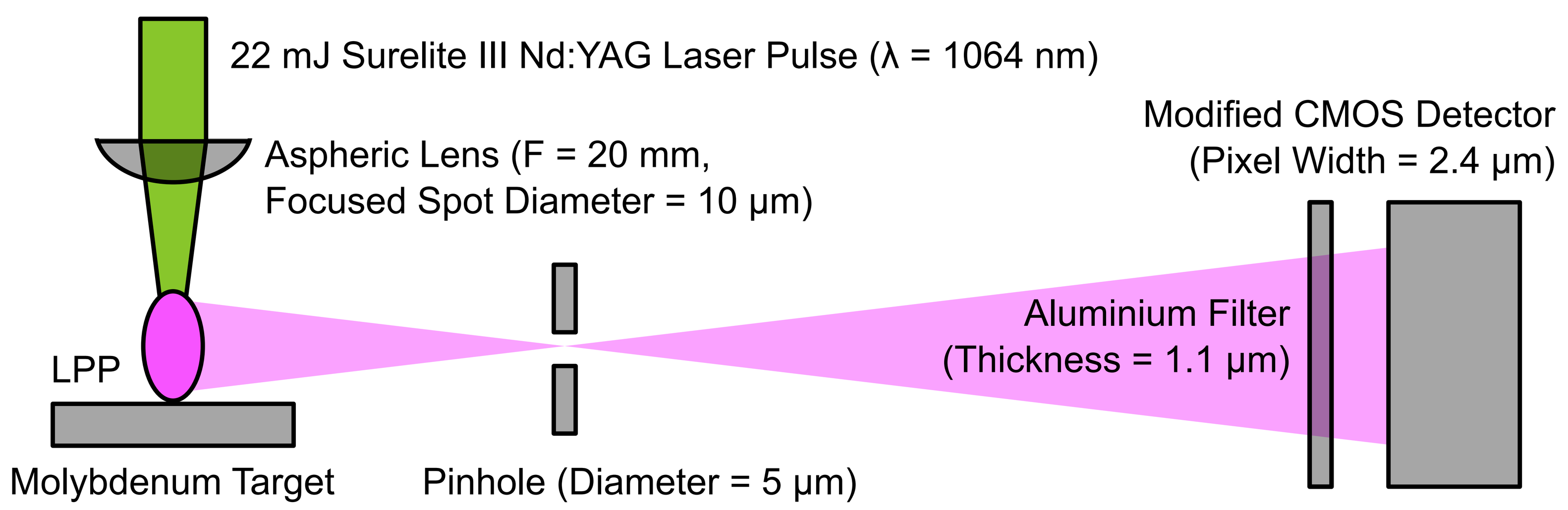

Fig. 1: Schematic of the experimental apparatus used to image SXR emission region of a LPP.

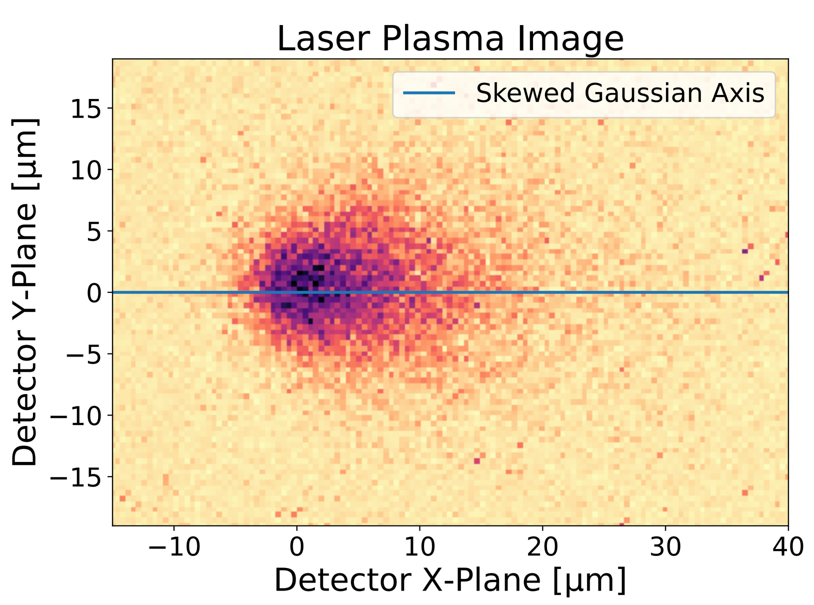

Fig. 2 (a): The mean average of five plasma images recorded at the experimental parameters listed in Fig. 1. This reduces the impact of the large signal to noise ratio present in the detector for low flux images.

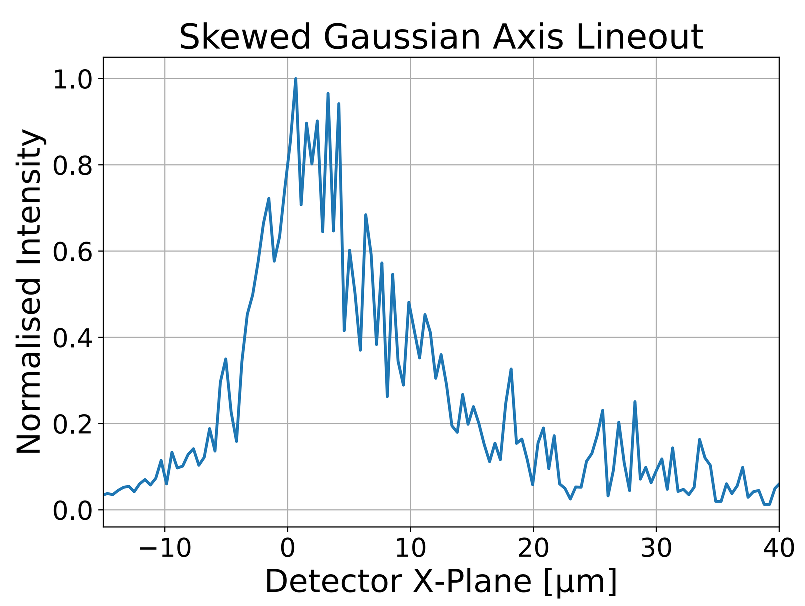

Fig. 2 (b): The normalised intensity lineout along the skewed Gaussian axis of the plasma image shown in Fig. 2 (a). Detector coordinates have been scaled down using a system magnification of 5.45.

[1] Gladson Joseph et al. "Laser plasma imaging and spectroscopy to enhance radiance for water window source development." In: Nuclear Instruments and Methods in Physics Research Section B: Beam Interactions with Materials and Atoms 482 (Nov. 2020), pp. 64–69.
[2] R.E. Burge et al. "Incoherent imaging with the soft x-ray microscope." In: Ultramicroscopy 83.1-2 (May 2000), pp. 75–92.

2. LPP Image Deconvolution

As illustrated in Fig. 1, an image of the source was projected onto the detector plane using a pinhole. During this process, light emitted by the source is diffracted at the pinhole according to the Huygens-Fresnel principle. This distorts the shape of the source recorded by the detector. Noise present in the system further degrades any recorded signal. The convolution theorem, expressed below, defines the mathematical model governing this image formation process.

$$\text{Image} = \text{Object} \circledast \text{PSF} + \text{Noise}$$

The point spread function (PSF) defines the degree to which an object's image is distorted by an imaging system. The object function is restored here by reversing the impact of noise and deconvolving this image with a modelled PSF of the system.

2.1 Point Spread Function Model

The PSF of the imaging system was modelled using the Fresnel diffraction integral (FDI). The FDI, expressed below, models the diffraction pattern created by waves passing through an aperture when observed from relatively close to the object.

$$E(x,y,Z_2) \cong -\frac{i e^{ikZ_2} e^{i\frac{k}{2Z_2}(x^2+y^2)}}{\lambda Z_2} \iint_{ap.} E(\xi,\eta,Z_1) e^{i\frac{k}{2Z_2}(\xi^2+\eta^2)} e^{-i\frac{k}{z}(x\xi+y\eta)} \, d\xi d\eta$$

The FDI was implemented in the model using the one-step propagation method outlined by Schmidt [3]. The PSF of the system is calculated using the modelled electric field, $E(x, y, Z_2)$.

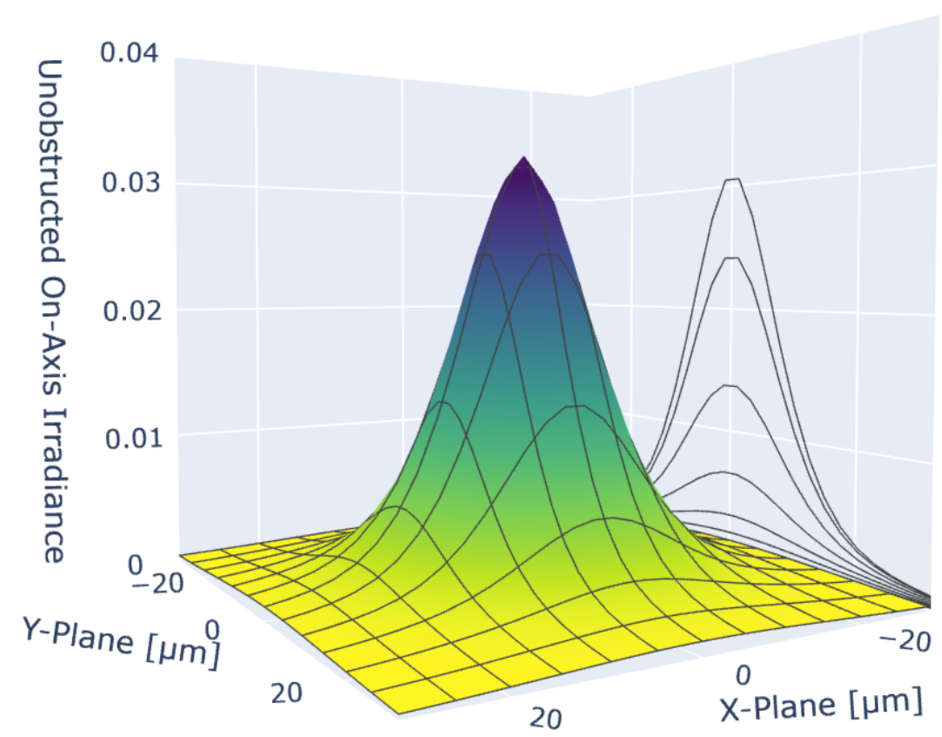

Fig. 3: The modelled PSF of the imaging system shown in Fig. 1. 1400 PSFs between 0.2 and 14.2 nm were modelled and weighted with respect to the relative flux of their wavelength received by the detector. These PSFs were summed together to produce the PSF shown.

[3] Jason D. Schmidt. Numerical Simulation of Optical Wave Propagation. SPIE, 2010. isbn: 9780819483263.

2.2 Noise Reduced Image Model

The plasma image shown in Fig. 2 (a) was simulated using a pseudo-voigt profile combined with regression techniques to produce a noise reduced image. This simulated plasma image is shown in Fig. 4 (a).

Results

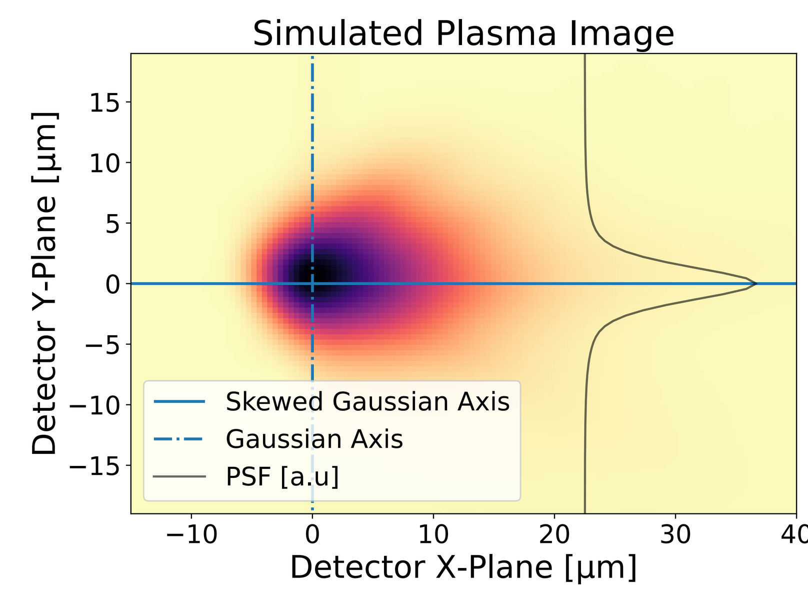

Fig. 4 (a): Simulated plasma image of plasma image shown in Fig. 2 (a). The PSF shown in Fig. 3 is also shown here for scale.

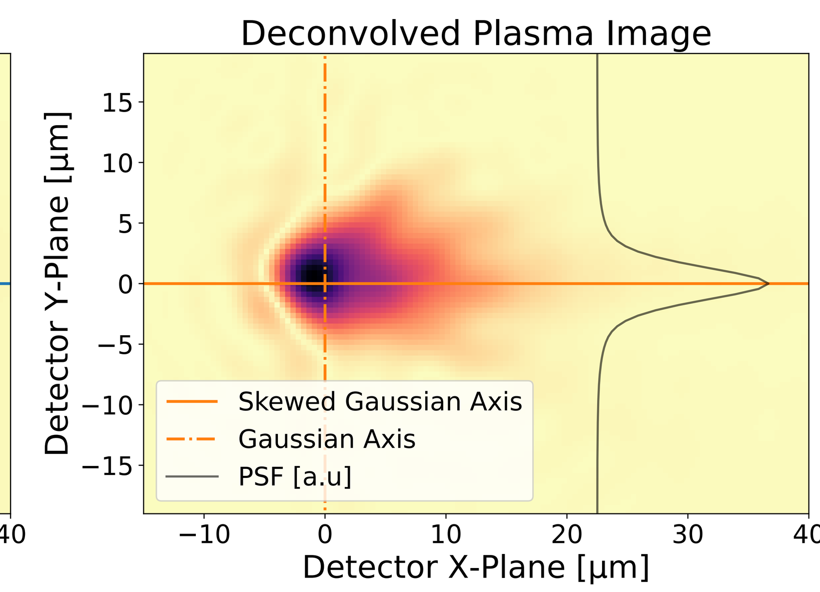

Fig. 4 (b): Deconvolved plasma image. The simulated plasma image shown in Fig. 4 (a) was deconvolved with PSF shown for scale.

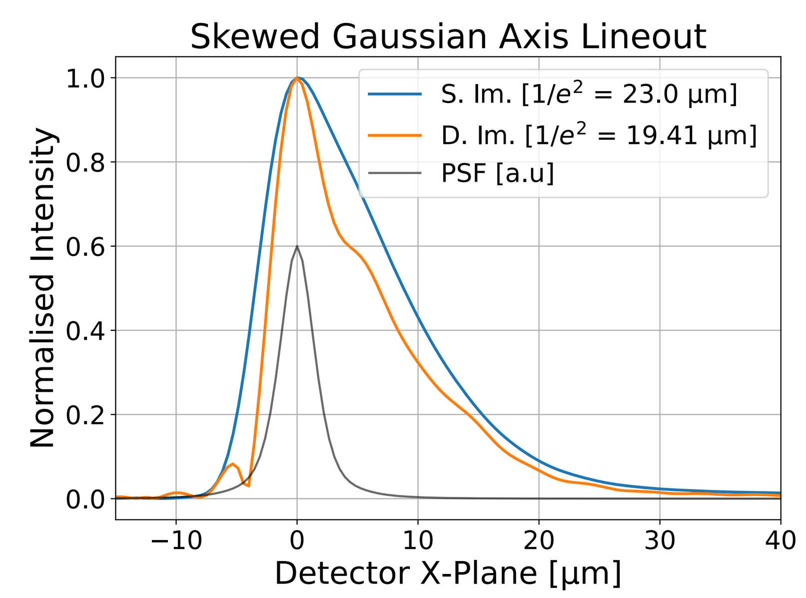

Fig. 4 (c): Normalised intensity lineouts along the skewed Gaussian axis of the simulated (blue) and deconvolved (orange) plasma images shown in Fig. 4 (a) and (b), respetively.

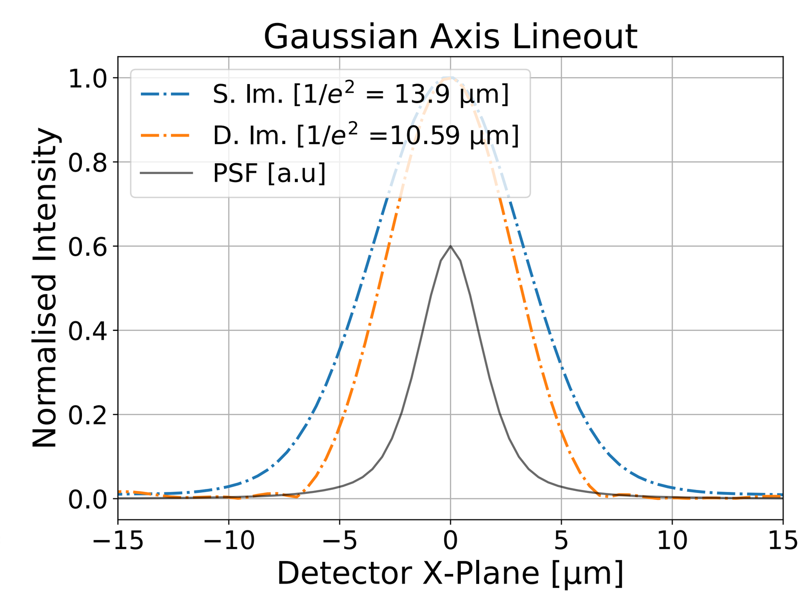

Fig. 4 (d): Normalised intensity lineouts along the Gaussian axis of the simulated (blue) and deconvolved (orange) plasma images shown in Fig. 4 (a) and (b), respectively.

The noise reduced simulated plasma image is deconvolved with the PSF of the imaging system. The deconvolved plasma image is shown in Fig. 4 (b). A 16.93% decrease along the skewed Gaussian axis is observed at the $1/e^2$ width for the deconvolved image. Similarly, a 27.03% difference is observed along the Gaussian axis. Furthermore, a 47.30% difference in plasma area above the $1/e^2$ width is observed between the simulated and deconvolved images. Future work will adopt this model to measure the radiance of sources whose SXR emission volumes are further reduced than those discussed in this presentation.

This work is supported by **Science Foundation Ireland** through a Frontiers for the Future Programme Award (**19/FFP/6795**).